arXiv:0704.2611v1 [cond-mat.mes-hall] 19 Apr 2007

Coulomb drag as a measure of trigonal warping in doped graphene

B.N. Narozhny
The Abdus Salam ICTP, Strada Costiera 11, Trieste, I-34100, Italy

(Dated: February 1, 2008)

I suggest to use the effect of Coulomb drag between two closely positioned graphite monolayers (graphene sheets) for experimental measurement of the strength of weak non-linearities of the spectrum in graphene. I consider trigonal warping as a representative mechanism responsible for the drag effect. Since graphene is relatively defect-free, I evaluate the drag conductivity in the ballistic regime and find that it is proportional to the fourth power of the warping strength.

The first experimental measurement of conducting properties of graphene [1] (an atomically thin crystalline monolayer of graphite) was followed by developing graphene-based transistors [2, 3], where high concentrations of charge carriers can be induced by applying gate voltages. These discoveries have brought a lot of attention to the field, which is well-studied theoretically. Indeed, a two-dimensional, hexagonal lattice of carbon atoms is a usual starting point for most calculations on bulk graphite, carbon nanotubes [4], or fullerenes [5]. In fact it's been almost 60 years since the band structure of graphene has been first studied [6].

The continuous theoretical interest in graphene is due to the Dirac-type dispersion relation [7, 8] leading to a number of peculiar properties – from the Berry phase of electronic wavefunctions [9] to an anomalous Quantum Hall Effect [3]. The chiral nature of charge carriers in graphene is a consequence of its crystal structure. The honeycomb lattice contains two equivalent sublattices. Nearest-neighbor hopping between A and B sites results in formation of two energy bands which intersect near the corners of the hexagonal Brillouin zone [4]. Two inequivalent corners $K_\pm$ [10] define a valley index, specifying excitations around the Fermi energy (playing a role of a pseudospin). Close to the crossing points the spectrum is conical with the "light-speed" $v \approx 10^6$ m/s [2].

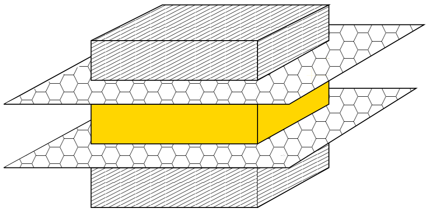

FIG. 1: A Coulomb drag sample: two graphene sheets are separated by an insulating layer of the thickness d. The two gates at the top and bottom of the device can be used to independently control carrier concentrations in the two sheets.

The true microscopic Hamiltonian in graphene contains several small corrections to the Dirac spectrum. For example, using a second order $\mathbf{k}\cdot\mathbf{p}$ equation [11] one can derive a quadratic term in the effective low-energy Hamiltonian of graphene that violates the isotropy of the Dirac spectrum and causes trigonal warping [9]. When gate voltage is applied, resulting in non-zero Fermi energy, the electronic Fermi line deviates from a perfect circle: the $\mathbf{p} \to -\mathbf{p}$ symmetry of the Fermi surface is broken within each valley. Although weak, such distortions of the Fermi surface lead to observable effects: trigonal warping suppresses antilocalization [12], which one would otherwise expect due to the absence of backscattering [9, 13].

Trigonal warping also breaks another, more subtle symmetry in the problem – the symmetry between excitations above and below the finite Fermi energy $E_F = \hbar v \sqrt{\pi n_e}$ (n_e being the electron density). Such asymmetry can be detected in transport measurements. A particular "tell-tale" experiment that crucially depends on its presence is Coulomb drag [14, 15, 16, 17, 18, 19, 20]. Coulomb drag measurements are performed on two closely positioned (but electrically isolated) layers. A current I_a driven through one of the layers (the "active" layer) induces a voltage drop $V_p = \rho_D I_a$ in the other ("passive") layer. The voltage appears due to inter-layer electron-electron interaction that creates a frictional force "dragging" electrons in the passive layer. As a purely interaction effect, Coulomb drag has become a sensitive tool for experimental studies of electron-electron interaction in many problems of contemporary condensed matter physics. It has been used in search for Bose condensation of interlayer excitons [21], a metal-insulator transition in two-dimensional layers [22], and Wigner cristallization in quantum wires [23].

Other effects contributing to non-linearity of the spectrum in graphene will also result in non-zero contribution to the Coulomb drag. These include: the quadratic correction to quasiparticle spectrum due to next-neighbor hopping [4]; Coulomb scatterers resulting in energy-dependent scattering time $\tau_c \propto |E_F|$ [24]; logarithmic corrections to quasiparticle spectrum [25]; and interference corrections to scattering time [26]. In this Letter I consider trigonal warping as a representative mechanism of the Coulomb drag in graphene, leaving the discussion of the role of other mechanisms for a subsequent publication [27]. I argue that this effect can be distinguished from other drag mechanisms by its dependence on interlayer separation d and Fermi momenta (or gate voltages).

I envision a following set-up (see Fig. 1). Two graphene sheets are positioned parallel to each other and are separated by an insulating material about 50 nm thick (e.g. using the technique recently developed in Ref. 28). Two gates (at the top and bottom of the device) can be used to independently control carrier concentrations in the two layers. I assume that sufficient gate voltage is applied, so that Fermi energies in each layer are positive $E_F^{(a,p)} > 0$ and represent the largest energy scale in the problem (indices a and p denote the active and passive layers). Since graphene is relatively defect-free, the elastic scattering rate τ^{-1} is assumed to be much smaller than temperature. At the same time, the mean-free path ℓ is the longest length scale. The assumed hierarchy of energy and length scales (here λ_F is the Fermi wavelength)

$$\hbar\tau^{-1} \ll T \ll E_F^{(a,p)}, \quad \ell^{(a,p)} \gg d \gg \lambda_F^{(a,p)}, \tag{1}$$

ensures that the the device is in the ballistic regime [29] (for Coulomb drag in the ballistic regime see Ref. 19).

At lower temperatures ($T < \hbar\tau^{-1}$) electron motion becomes diffusive. In that case, scattering off atomically sharp disorder becomes important for it breaks the pseudospin symmetry and drastically affects two-particle correlation functions [12]. An analysis of the Coulomb drag in the diffusive regime will be considered elsewhere [27].

In the weak coupling regime [18, 19, 20] the drag coefficient is proportional to the drag conductivity $\rho_D \approx \sigma_D/(\sigma_a\sigma_p)$ ($\sigma_{(a,p)}$ being the Drude conductances of the two layers). The latter is typically calculated using the expresssion

$$\sigma_D^{\beta\beta'} = \frac{1}{8TS}\sum_{\mathbf{q}}\int\frac{d\omega}{2\pi}\left|\mathcal{D}_{ap}\right|^2\frac{\Gamma_a^{\beta}(\omega,\mathbf{q})\Gamma_p^{\beta'}(\omega,\mathbf{q})}{\sinh^2\frac{\omega}{2T}}, \tag{2}$$

where S is the sample area, $\mathcal{D}_{ap}$ is the screened interlayer interaction, and $\mathbf{\Gamma}$ is the non-linear susceptibility (or rectification function) that relates a scalar potential $V(\omega,\mathbf{q})$ to the *dc* current it creates in quadratic response $\mathbf{j}_{dc} = \mathbf{\Gamma}(\omega,\mathbf{q})|V(\omega,\mathbf{q})|^2$. Below I re-derive Eq. (2) for graphene in the ballistic regime under the above assumptions and show, that for Dirac particles the drag vanishes.

When trigonal warping is taken into account, I find that the drag conductivity is proportional to the fourth power of the parameter W that describes the strength of the warping correction to the Dirac spectrum:

$$\sigma_D = \frac{e^2}{\hbar}\frac{5\zeta[5]}{32}\frac{\hbar^2}{(\kappa_a d)(\kappa_p d)}\frac{T^2W^4}{v^6d^2}\frac{\ell_a\ell_p}{d^2}. \tag{3}$$

Here $\kappa_{(a,p)} = e^2k_F^{(a,p)}/v$ are the Thomas-Fermi momenta. Eq. (3) is the main result of this communication.

The low-energy single-particle Hamiltonian [7, 9, 12] in graphene can be written in the basis of 4-component Bloch functions $\Phi = (\phi_{A,K_+}, \phi_{B,K_+}, \phi_{B,K_-}, \phi_{A,K_-})$ (I employ notations introduced in Ref. 12; ϕ_{A,K_+} is the electronic amplitude on sublattice A and valley K_+) as

$$\widehat{\mathcal{H}}_0 = v\vec{\Sigma}\mathbf{p} - W\Big[\hat{\sigma}_x\left(p_x^2 - p_y^2\right) - 2\hat{\sigma}_y p_x p_y\Big], \tag{4}$$

with the weak quadratic term causing trigonal warping. Here Pauli matrices $\hat{\sigma}_i$ act in the sublattice space (A, B). The "isospin" $\vec{\Sigma}$ is defined as direct products of Pauli matrices $\hat{\sigma}$ (acting in the sublattice space) and $\mathbf{\Pi}$ (acting in the valley space $K_\pm$): $\Sigma_{x(y)} = \Pi_z \otimes \hat{\sigma}_{x(y)}$.

In the basis of plane waves $\widehat{\mathcal{H}}_0$ is a 4×4 matrix that can be diagonalized by a unitary transformation $\hat{R}^{-1}\widehat{\mathcal{H}}_0\hat{R} = \mathrm{diag}[E_{\alpha,\xi}(\mathbf{p})]$. The resulting eigenvalues are

$$E_{\alpha,\xi} = \alpha v p s_\xi; \; s_\xi = \sqrt{1 - 2\xi pWv^{-1}\cos 3\varphi_{\mathbf{p}} + p^2W^2v^{-2}}, \tag{5}$$

where $\xi = \pm1$ denotes the two valleys, $\alpha = \pm1$ is the chirality and distinguishes between the conductance ($\alpha = 1$) and valence ($\alpha = -1$)bands, and $\varphi_{\mathbf{p}}$ is an angle between the momentum $\mathbf{p}$ and the x-axis ($\tan\varphi_{\mathbf{p}} = p_y/p_x$).

The electron field operator can be written in the basis of the eigenstates as (hereafter I use the units with $\hbar = 1$)

$$\widehat{\Psi}(\mathbf{r}) = \sum_{\mathbf{p},\alpha,\xi}\psi_{\mathbf{p},\alpha,\xi}(\mathbf{r})\widehat{a}_{\mathbf{p},\alpha,\xi} = \frac{1}{\sqrt{2}}\sum_{\mathbf{p},\alpha}e^{i\mathbf{pr}}\begin{pmatrix} e_{\alpha,\xi=1} \\ 1 \\ 0 \\ 0 \end{pmatrix}\widehat{a}_{\mathbf{k},\alpha,\xi=1} + \frac{1}{\sqrt{2}}\sum_{\mathbf{p},\alpha}e^{i\mathbf{pr}}\begin{pmatrix} 0 \\ 0 \\ e_{\alpha,\xi=-1} \\ 1 \end{pmatrix}\widehat{a}_{\mathbf{p},\alpha,\xi=-1}, \tag{6}$$

where $e_{\alpha,\xi} = \alpha s_\xi e^{2i\varphi_p}/[e^{3i\varphi_p} - (\xi pW/v)]$. Then the form of the electron density operator

$$\widehat{\rho}(\mathbf{r}) = \sum_{\mathbf{p},\mathbf{p}',\alpha,\alpha',\xi} e^{-i(\mathbf{p}-\mathbf{p}')\mathbf{r}}\widehat{a}^\dagger_{\mathbf{p},\alpha,\xi}\widehat{a}_{\mathbf{p}',\alpha',\xi}\lambda^{\alpha,\alpha'}_{\mathbf{p},\mathbf{p}'}, \tag{7}$$

differs from the usual one by the presence of vertices

$$\lambda^{\alpha,\alpha'}_{\mathbf{p},\mathbf{p}'} = \left(1 + e_{\alpha,\xi}e^*_{\alpha',\xi}\right)/2. \tag{8}$$

The vertices $\lambda^{\alpha,\alpha'}_{\mathbf{k},\mathbf{k}'}$ indicate the asymmetry of quasiparticle scattering in graphene. In particular, the supression of backscattering [9] follows from the fact that in the absence of trigonal warping $\lambda^{\alpha,\alpha}_{\mathbf{p},-\mathbf{p}}(W = 0) = 0$. Similarly, $\lambda^{\alpha,-\alpha}_{\mathbf{p},\mathbf{p}}(W = 0) = 0$, indicating that inter-band transitions at the same wave-vector are also supressed.

The single-particle Green's function in the original basis of Bloch functions is a 4×4 matrix [12] It can be brought to a diagonal form by the rotation $\hat{R}$. In any closed loop such operation would cause the appearance of the vertex factors (8). For example, the polarization operator (the density-density response function) is

$$\mathcal{P}_0(\omega, \mathbf{q}) = -2i \sum_{\alpha,\alpha',\xi} \int \frac{d^2k}{(2\pi)^2} \int \frac{d\epsilon}{2\pi} \qquad (9)$$

$$\times \left|\lambda^{\alpha,\alpha'}_{\mathbf{k},\mathbf{k}+\mathbf{q}}\right|^2 G_{\alpha,\xi}(\epsilon, \mathbf{k})\, G_{\alpha',\xi}(\epsilon + \omega, \mathbf{k} + \mathbf{q}),$$

where the overall factor of 2 follows from the spin degeneracy. Here $G_\alpha(\epsilon, \mathbf{k})$ is the Green's function for the α band. For $E_F > 0$ and $T \ll E_F$ one can use the standard non-relativistic Green's functions [30].

Since the vertex functions are frequency-independent, the usual reasoning [31] leads to the following expression for the retarded polarization operator in the ballistic regime ($f[E_\alpha(\mathbf{k})]$ is the Fermi function)

$$\mathcal{P}^R_0(\omega, \mathbf{q}) = -2 \sum_{\alpha,\alpha',\xi} \int \frac{d^2k}{(2\pi)^2} \qquad (10)$$

$$\times \left|\lambda^{\alpha,\alpha'}_{\mathbf{k},\mathbf{k}+\mathbf{q}}\right|^2 \frac{f[E_{\alpha',\xi}(\mathbf{k}+\mathbf{q})] - f[E_{\alpha,\xi}(\mathbf{k})]}{\omega - E_{\alpha',\xi}(\mathbf{k}+\mathbf{q}) + E_{\alpha,\xi}(\mathbf{k}) + i\eta},$$

where $\eta \to +0$. Note, that under assumptions that the Fermi level is in the conduction band and $T \ll E_F$, the term with $\alpha = \alpha' = -1$ (the valence band contribution) vanishes due to the Fermi functions.

For the purposes of describing screened inter-layer interaction in the Coulomb drag problem, I am only interested in momenta q smaller than inverse inter-layer distance. Under the assumption (1), $q < (1/d) \ll k_F$. Thus, the inter-band contribution to Eq. (10) is suppressed by a factor of q^2/k_F^2 and the polarization operator is dominated by the conduction band. Due to the Fermi functions in Eq. (10) the momentum integral is dominated by the region $k \sim k_F$. Then the leading contribution to the static polarization operator needed in the Coulomb drag problem in the ballistic regime [19] is

$$\mathcal{P}^R_0(\omega = 0) = 2k_F/\pi v = 4\nu. \qquad (11)$$

Here ν is the density of states at the Fermi level (spin and valley degeneracy is taken into account). Consequently, the screened interlayer interaction is the same as in the case of the uniform two-dimensional electron gas [19]:

$$\mathcal{D}_{ab} = \pi e^2 q/(\kappa_a \kappa_p \sinh qd). \qquad (12)$$

To derive the expression for the drag conductivity (2) one starts with the general expression for electric current in the passive layer in terms of the Keldysh Green's function. In graphene the current vertex (in the original basis of Bloch functions) is $\hat{\mathbf{J}} = 2ev\vec{\Sigma}$. Diagonalizing the Green's function by a unitary transformation the current in the passive layer takes the form

$$\mathbf{j} = -\frac{i}{2S} \sum_{\alpha,\xi} \int d^d r \hat{\mathbf{j}}_{\alpha,\xi} G^K_{\alpha,\xi};\ \hat{\mathbf{j}}_{\alpha,\xi} = \left(\hat{R}^{-1}\hat{\mathbf{J}}\hat{R}\right)^{\xi,\xi}_{\alpha,\alpha}. \qquad (13)$$

In a system of free electrons in equilibrium the current (13) is equal to zero. Perturbing the Green's function by a potential $V(\omega)$ one finds the following expression for the current [more precisely, the contribution relevant for the drag problem; here I use a short-hand notation for the spatial coordinates in the argument of Green's functions – $G^R_{\alpha,\xi}(\epsilon; 31) = G^R_{\alpha,\xi}(\epsilon; \mathbf{r}_3, \mathbf{r}_1)$]

$$\mathbf{j} = \frac{i}{V} \sum_{\alpha,\xi} \int d^d r_3 \int \frac{d\epsilon}{2\pi} \frac{d\omega}{2\pi} \Big(f[\epsilon] - f[\epsilon - \omega] \Big) V(\omega; 12) \left[\sum_{\alpha'} \mathrm{Im} G^R_{\alpha',\xi}(\epsilon - \omega; 12) \left|\lambda^{\alpha,\alpha'}\right|^2 \right] G^A_{\alpha,\xi}(\epsilon; 23) \hat{\mathbf{j}}_{\alpha,\xi} G^R_{\alpha,\xi}(\epsilon; 31). \qquad (14)$$

In the ballistic regime [19] Green's functions in Eq. (14) are averaged over the disorder independently of each other. Then one can perform the Fourier transform and use the approximation (τ is the elastic scattering rate):

$$G^R_{\alpha,\xi}(\epsilon; \mathbf{k}) G^A_{\alpha,\xi}(\epsilon; \mathbf{k}) \approx 2\pi\tau\delta\Big(\epsilon - E_{\alpha,\xi}(\mathbf{k})\Big), \qquad (15a)$$

$$\mathrm{Im} G^R_{\alpha,\xi}(\epsilon; \mathbf{k}) \approx -\pi\delta\Big(\epsilon - E_{\alpha,\xi}(\mathbf{k})\Big). \qquad (15b)$$

In this case

$$f[\epsilon] - f[\epsilon - \omega] \to f[E_{\alpha,\xi}(\mathbf{k})] - f[E_{\alpha,\xi}(\mathbf{k} - \mathbf{q})].$$

It is then clear that if the Fermi level is in the conduction band then the two Fermi functions for the valence bands cancel each other. Inter-band processes are suppressed similarly to the case of the polarization operator and will be neglected hereafter. Thus, in the ballistic regime, only particles in the conduction band contribute to the current in the passive layer, as one would intuitively assume. The question of whether this statement remains true when off-diagonal disorder is taken into account, i.e. in the diffusive regime, will be discussed in a subsequent publication [27]. The situation in the active layer is similar, in fact both layers are described by the same non-linear susceptibility $\mathbf{\Gamma}$. Therefore, the general expression for the drag conductivity (2) remains valid (again, with only particles in the conduction band contributiong). What remains to be done inorder to obtain the result (3) is to evaluate the non-linear susceptibility.

Under my assumptions the non-linear susceptibility for the conduction band in the ballistic regime is

$$\mathbf{\Gamma}(\omega,\mathbf{q}) = \frac{\omega}{\pi}\left[\vec{\gamma}_{\mathbf{q}}(\omega) - \vec{\gamma}_{-\mathbf{q}}(-\omega)\right], \tag{16}$$

where the triangular vertex $\vec{\gamma}$ is given by

$$\vec{\gamma}_{\mathbf{q}}(\omega) = \sum_{\xi}\int\frac{d^2k}{(2\pi)^2}\left|\lambda^{1,1}_{\mathbf{k},\mathbf{k}+\mathbf{q}}\right|^2 \tag{17}$$
$$\times\Big[\mathrm{Im}G^R_{1,\xi}(\epsilon+\omega;\mathbf{k}+\mathbf{q})\Big]G^R_{1,\xi}(\epsilon;\mathbf{k})\,\hat{\mathbf{j}}_1 G^A_{1,\xi}(\epsilon;\mathbf{k}).$$

Here $\hat{\mathbf{j}}_1$ is the diagonal matrix element of the curent vertex $\widehat{\mathbf{J}}$ rotated (13) to the basis of the eigenfunctions: $\hat{\mathbf{j}}_1 = 2ev\mathbf{n}_{\mathbf{k}}$. Note how the current vertex for the conduction band recovers its usual momentum dependence!

Consider now the Coulomb drag for Dirac particles. Setting $W = 0$ in Eq. (8), one finds $[\theta = \angle(\mathbf{k},\mathbf{q})]$

$$\gamma^{\beta} = -4ev_F\pi\nu\tau_0\int\frac{d\theta}{2\pi}n^{\beta}_{\mathbf{k}}\left(1-\frac{q^2}{4k^2}\sin^2\theta\right) \tag{18}$$
$$\times\delta\Big(\omega - E_1(\mathbf{k}+\mathbf{q}) + E_1(\mathbf{k})\Big).$$

The result is even under the simultaneous change of sign of ω and $\mathbf{q}$: $\vec{\gamma}_{\mathbf{q}}(\omega) = \vec{\gamma}_{-\mathbf{q}}(-\omega)$. Therefore $\mathbf{\Gamma}(\omega,\mathbf{q}) = 0$. There is no drag effect in a system with linear spectrum.

When the deviation from linearity in Eq. (4) is taken into account, the contribution of the two valleys to Eq. (18) is no longer identical and a non-zero result appears only in the second order in W:

$$\mathbf{\Gamma}(\omega,\mathbf{q}) = -4e\nu\mathbf{q}\omega w^2\ell v^{-3}\sin\varphi_{\mathbf{q}}\cos 3\varphi_{\mathbf{q}}\theta(vq-\omega), \tag{19}$$

where the mean-free path is defined as $\ell = 2v\tau$. Using Eqs. (19) and (12) in Eq. (2), I find the final result (3).

To summarize, I have considered the Coulomb drag between two closely positioned graphene sheets. For strictly linear Dirac-type dispersion, I find that the drag vanishes, in agreement with the traditional interpretation of the effect as a manifestation of asymmetry between elementary excitations above and below the Fermi level. As a representative mechanism of such asymmetry in graphene I consider trigonal warping and find the drag coefficient proportional to the fourth power of the strength W of the warping term [32]. The obtained result should be distinguishable from the drag due to other non-linear contributions [4, 24, 25, 26] to graphene spectrum by its dependence on inter-layer separation and Fermi momentum. In my opinion the Coulomb drag is an ideal tool for experimental studies of spectrum non-linearities in graphene.

I am grateful to V.I Fal'ko for attracting my attention to this problem, to I.L. Aleiner for helpful discussions and to MPI-PKS, Dresden for hospitality during the workshop "Dynamics and Relaxation in Complex Quantum and Classical Systems and Nanostructures" (2006).

[1] K.S. Novoselov *et al.*, Science **306**, 666 (2004).
[2] K.S. Novoselov *et al.*, Nature **438**, 197 (2005).
[3] Y. Zhang *et al.*, Nature **438**, 201 (2005).
[4] R. Saito, G. Dresselhaus, M.S. Dresselhaus, *Physical Properties of Carbon Nanotubes* (Imperial College, London, 1998).
[5] R.F. Curl, Rev. Mod. Phys. **69**, 691 (1997); H. Kroto, *ibid* **69**, 703 (1997); R.E. Smalley, *ibid* **69**, 723 (1997).
[6] P.R. Wallace, Phys. Rev. **71**, 622 (1947).
[7] J.C. Slonczewski and P.R. Weiss, Phys. Rev. **109**, 272 (1958).
[8] G.W. Semenoff, Phys. Rev. Lett. **53**, 2449 (1984).
[9] T. Ando, T. Nakanishi, and R. Saito, J. Phys. Soc. Jpn. **67**, 2857 (1998).
[10] The two inequivalent corners of the Brillouin zone $K_{\pm}$ are $(\pm\frac{4}{3}\pi a^{-1}, 0)$, where a is the lattice constant.
[11] H. Ajiki and T. Ando, J. Phys. Soc. Jpn. **65**, 505 (1996).
[12] E. McCann *et.al.*, Phys. Rev. Lett. **97**, 146805 (2006); K. Kechedzhi *et.al.*, cond-mat/0701690.
[13] S. Hikami, A.I. Larkin, and N. Nagaosa, Prog. Theor. Phys. **63**, 707 (1980).
[14] P. M. Solomon *et al.*, Phys. Rev. Lett. **63**, 2508 (1989).
[15] T. J. Gramila *et al.*, Phys. Rev. Lett. **66**, 1216 (1991).
[16] M.B. Pogrebinskii, Fiz. Tekh. Poluprovodn. **11**, 637 (1977) [Sov. Phys. Semicond. **11**, 372 (1977)].
[17] P.M. Price, Physica (Amsterdam) **117B**, 750 (1983).
[18] L. Zheng and A.H. MacDonald, Phys. Rev. B **48**, 8203 (1993).
[19] A. Kamenev and Y. Oreg, Phys. Rev. B **52**, 7516 (1995).
[20] K. Flensberg *et al.*, Phys. Rev. B **52**, 14761 (1995).
[21] D. Snoke, Science **298**, 1368 (2002).
[22] R. Pillarisetty *et al.*, Phys. Rev. B **71**, 115307 (2005).
[23] M. Yamamoto *et al.*, Science **313**, 204 (2006).
[24] K. Nomura and A.H. MacDonald, Phys. Rev. Lett. **98**, 076602 (2007).
[25] A.A. Abrikosov and S.D. Beneslavskii, Sov. Phys. JETP **32**, 699 (1971); J. Gonzalez, F. Guinea, and M.A.H. Vozmediano, Phys. Rev. B **59**, R2474 (1999); D.T. Son, cond-mat/0701501.
[26] I. L. Aleiner and K. B. Efetov, Phys. Rev. Lett. **97**, 236801 (2006).
[27] B.N. Narozhny, unpublished.
[28] D. Goldhaber-Gordon *et al.*, unpublished.
[29] G. Zala, B.N. Narozhny, and I.L. Aleiner, Phys. Rev. B **64**, 214204 (2001); V.V. Cheianov and V.I. Fal'ko, Phys. Rev. Lett. **97**, 226801 (2006).
[30] S.A. Chin, Ann. Phys. **108**, 301 (1977).
[31] G. Mahan. *Many-Particle Physics*, Plenum, New York, 1990.
[32] I believe that the role of the symmetry between excitations above and below E_F was ovelooked in Ref. 33.
[33] I. D'Amico and S.G. Sharapov, cond-mat/0410769.